

The Topology of Three-Dimensional Symmetric Tensor Fields

Yingmei Lavin
Department of Physics
Stanford University
Stanford, CA 94305

Yuval Levy
Department of Aeronautics and Astronautics
Stanford University
Stanford, CA 94305-4035

Lambertus Hesselink
Department of Electrical Engineering
Stanford University
Stanford, CA 94305-4035

1 Abstract

We study the topology of 3-D symmetric tensor fields. The goal is to represent their complex structure by a simple set of carefully chosen points and lines analogous to vector field topology. The basic constituents of tensor topology are the degenerate points, or points where eigenvalues are equal to each other. First, we introduce a new method for locating 3-D degenerate points. We then extract the topological skeletons of the eigenvector fields and use them for a compact, comprehensive description of the tensor field. Finally, we demonstrate the use of tensor field topology for the interpretation of the two-force Boussinesq problem.

2 Introduction

Second-order tensor fields have applications in many areas of physics, such as general relativity, fluid flows and mechanical properties of solids. The wealth of multivariate information in tensor fields makes them more complex and abstract than scalar and vector fields. Visualization provides a means to gain new insights from these rich data sets.

The most natural way to visualize a symmetric 3-D tensor field is through its eigensystem, i.e., eigenvalues and eigenvectors. A continuous representation of the tensor field is obtained by tracing the trajectories of its eigenvectors. These trajectories are called hyperstreamlines [1, 2]. The difficulty with such an approach is how to capture the structure of the 3-D domain while limiting the number of hyperstreamlines to a minimum in order to avoid visual clutter. The problem can be significantly simplified by taking a topological approach, similar to the one used in visualizing vector fields [3]. Degenerate points, defined as points where eigenvalues are equal to each other, are the basic singularities underlying the topology of tensor fields. Eigenvectors never cross each other except at degenerate points. In

the past, research has been conducted in the area of two-dimensional tensor fields [1, 2]. We live, however, in a three-dimensional world, and therefore, it is important for us to understand the underlying physics of this world. In this paper, we describe a new method for locating degenerate points along with the conditions for classifying them in three-dimensional space. We also discuss some topological features of three-dimensional tensor fields, and interpret topological patterns in terms of physical properties.

3 Theoretical Background

3.1 Definitions

Definition 1 (Second-Order Tensor Field) Let $\mathcal{L}(X, Y)$ be the set of all the linear transformations of the vector space X into the vector space Y , and let E be an open subset of \mathbf{R}^n . A second-order tensor field $\mathbf{T}(\vec{x})$ defined across E is a mapping $\mathbf{T} : E \rightarrow \mathcal{L}(\mathbf{R}^m, \mathbf{R}^m)$ that associates to each vector \vec{x} of E a linear transformation of \mathbf{R}^m into itself. If \mathbf{R}^m is referenced by a Cartesian coordinate system, $\mathbf{T}(\vec{x})$ can be represented by m^2 Cartesian components $T_{ij}(\vec{x})$, $i, j = 1, \dots, m$, that transform according to

$$T'_{ij} = \sum_{p,q=1}^m \beta_{ip} \beta_{jq} T_{pq} \quad (1)$$

under an orthonormal transformation $\beta = \{\beta_{ij}\}$ of the coordinate axes. [2]

In a Cartesian coordinate system, a 3-D tensor field takes the following form:

$$\mathbf{T}(\vec{x}) = \begin{pmatrix} T_{11}(x, y, z) & T_{12}(x, y, z) & T_{13}(x, y, z) \\ T_{21}(x, y, z) & T_{22}(x, y, z) & T_{23}(x, y, z) \\ T_{31}(x, y, z) & T_{32}(x, y, z) & T_{33}(x, y, z) \end{pmatrix} \quad (2)$$

Definition 2 (Hyperstreamline) A geometric primitive of finite size sweeps along the longitudinal eigenvector field, \vec{v}_1 , while stretching in the transverse plane under the combined action of the two transverse eigenvectors, \vec{v}_{t1} and \vec{v}_{t2} . Hyperstreamlines are surfaces that envelop the stretched primitives along the trajectories. We refer to hyperstreamlines as “major”, “medium” or “minor” depending on the corresponding longitudinal eigenvector field that defines their trajectories and color hyperstreamlines by means of a user-defined function of the three eigenvalues, usually the amplitude of the longitudinal eigenvalue. [4]

Definition 3 A degenerate point of a tensor field $\mathbf{T} : E \rightarrow \mathcal{L}(\mathbf{R}^m, \mathbf{R}^m)$, where E is an open subset of \mathbf{R}^m , is a point $\vec{x}_0 \in E$ where at least two of the m eigenvalues of \mathbf{T} are equal to each other. [4]

3.2 Locating Degenerate Points

A three-dimensional symmetric tensor field (Equation (2)) has 6 independent variables, therefore various types of degenerate points may exist. These types correspond to the following conditions:

$$\lambda_1(\vec{x}_0) = \lambda_2(\vec{x}_0) > \lambda_3(\vec{x}_0) \quad (3)$$

$$\lambda_1(\vec{x}_0) > \lambda_2(\vec{x}_0) = \lambda_3(\vec{x}_0) \quad (4)$$

$$\lambda_1(\vec{x}_0) = \lambda_2(\vec{x}_0) = \lambda_3(\vec{x}_0) \quad (5)$$

The characteristic equation of a 3-D symmetric tensor can be expressed in the following form

$$\begin{aligned} A(\lambda) &= \begin{vmatrix} T_{11} - \lambda & T_{12} & T_{13} \\ T_{12} & T_{22} - \lambda & T_{23} \\ T_{13} & T_{23} & T_{33} - \lambda \end{vmatrix} \\ &= -\lambda^3 + a\lambda^2 + b\lambda + c \end{aligned} \quad (6)$$

where a , b and c are composed of the 6 independent tensor components. The condition for the existence of a degenerate point is that both $A(\lambda(\vec{x}_0))$ and its derivative $\frac{dA(\lambda(\vec{x}_0))}{d\lambda}$ are zero.

$$\begin{cases} A(\lambda(\vec{x}_0)) = -\lambda^3 + a\lambda^2 + b\lambda + c = 0 \\ \frac{dA(\lambda(\vec{x}_0))}{d\lambda} = -3\lambda^2 + 2a\lambda + b = 0 \end{cases} \quad (7)$$

As a result, we obtain the following conditions corresponding to Equations (3, 4, and 5) respectively:

$$B_1(x, y, z) = \frac{2a^3 + 9ab + 2d^{3/2}}{27} + c = 0 \quad (8)$$

$$B_2(x, y, z) = \frac{2a^3 + 9ab - 2d^{3/2}}{27} + c = 0 \quad (9)$$

$$B_3(x, y, z) = a^2 + 3b = 0 \quad (10)$$

From the expressions for B_1 , B_2 and B_3 , we determine that: $B_1(x, y, z) = 0$ is a maximum for B_1 , $B_2(x, y, z) = 0$ is a minimum for B_2 and $B_3(x, y, z) = 0$ is a maximum for B_3 .

Now the problem is to find extrema in a 3D continuous field from the discrete experimental data sets. On a 3-D discrete mesh, the search for the various extrema is conducted by processing one grid cell at a time for each spatial function.

This method can successfully locate the points of triple degeneracy. It is especially useful when extended to locate points of double degeneracy where the local tensor appears in the diagonal form only when transformed into its eigenvector space.

3.3 Separating Surfaces

For second order tensor fields, in most cases, the eigenvector fields in the vicinity of a degenerate point can be described in terms of three types of angular sectors: hyperbolic, parabolic and elliptic sectors. It can be proved that in a 2-D tensor field, at a simple degenerate point, there are only one or three hyperbolic sectors, and no elliptic sectors [2]. Correspondingly, we call the degenerate point a wedge point when it has only one hyperbolic sector and possibly one parabolic sector or a trisector point when it has three hyperbolic sectors [2].

The classification of degenerate points in 2-D tensor fields [2, 5] can then be extended to 3-D tensor fields. The building blocks are the fundamental elements as defined for 2-D [2]. However, the separating surfaces in 3-D tensor fields have a general structure as they could appear at various angles. Each of the surfaces is characterized by patterns similar to those of hyperbolic or parabolic sectors and is bounded by hyperstreamlines that are emanating from or terminated at the degenerate point. Consequently, a point of triple degeneracy can be classified by the number and type of separating surfaces surrounding it.

In Figure 1 we show the eigenvector patterns in the vicinity of a point of triple degeneracy with 4 bounding hyperstreamlines. These hyperstreamlines form 6 hyperbolic separating surfaces. Figure 2 shows a point of triple degeneracy with only 3 bounding hyperstreamlines which form 2 hyperbolic separating surfaces and one parabolic surface.

The trajectories on the surfaces are locally 2-D, while off the surfaces they are fully 3-D and are determined by their closest surface.

4 Topology of 3-D Tensor Fields

We choose the elastic stress tensor induced by two compressive forces on the top of a semi-infinite

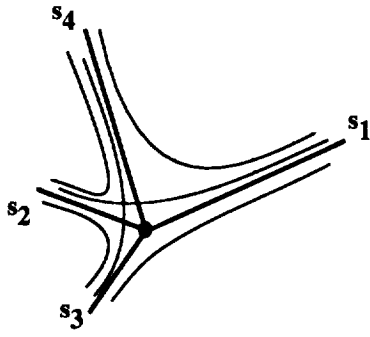


Figure 1: A point of triple degeneracy with 6 hyperbolic separating surfaces.

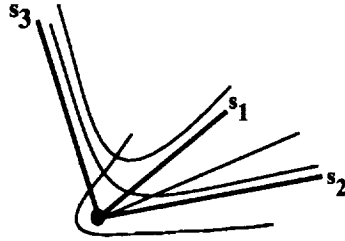


Figure 2: A point of triple degeneracy with 2 hyperbolic separating surfaces and one parabolic surface.

plane [6] to illustrate the advantages of using topological skeletons in visualizing 3-D tensor fields. In principle, hyperstreamline trajectories of the stress tensor show the transmission of forces inside the material. Figure 3 shows two hyperstreamlines corresponding to the most compressive eigen-direction, the minor eigenvector \bar{v}_3 . The two forces, indicated by the arrows, act on the surface at $P_1 = (0.5, 0.0, -1.05)$ and $P_2 = (-0.5, 0.0, -1.05)$ in the $+z$ direction (downward). The domain of interest (described by the bounding frame) extends between $(-1.0, -1.0, -1.114367)$ and $(1.0, 1.0, 0.0)$ so it includes the key features of the stress tensor field, i.e., the degenerate points. It is assumed that the region where $z < -1.05$ is in tension and that no stresses are transferred across the plane $z = -1.05$. The color of the hyperstreamlines encodes the magnitude of the most compressive eigenvalue, λ_3 , while their cross section encodes the magnitude and direction of the transverse eigenvectors. The hyperstreamlines converge toward regions of high stresses where the forces are applied. Note the sharp change in color and cross section size of the hyperstreamlines as they approach the acting points of the forces.

Analysis reveals that the tensor field contains two points of triple degeneracy and that these points reside on the surface of the semi-infinite plane. Moreover, the eigenvalues at these points (the location of which is given by: $D_1 = (0.0, 0.5, -1.05)$, $D_2 = (0.0, -0.5, -1.05)$) are equal to zero. This means that



Figure 3: Stress tensor induced by two compressive forces; minor hyperstreamlines

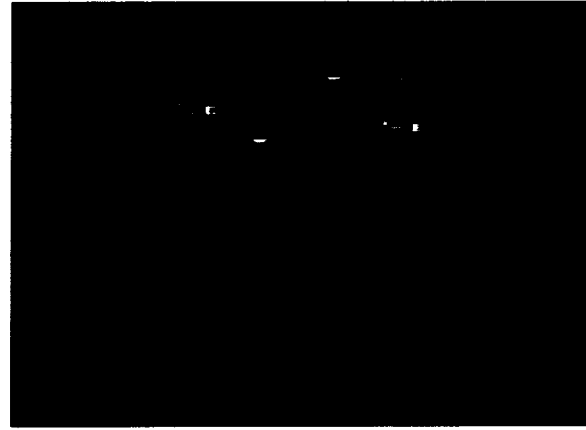


Figure 4: Stress tensor induced by two compressive forces; major hyperstreamlines

these points are stress free, a fact that can be verified by an examination of the stress equations. We have therefore acquired physical insight into the stress tensor field just by examining a basic topological feature, a point of triple degeneracy.

Figure 4 shows hyperstreamlines that are obtained by tracing the major eigenvector field. The location and direction of the forces are indicated by the arrows and the location of the points of triple degeneracy are marked by spheres. The hyperstreamlines are presented with a constant cross section to avoid visual clutter resulting from the high eigenvalues in the vicinity of the points of the acting forces. They are, however, still color encoded by the major eigenvalue. Each of the 2 degenerate points has 4 bounding hyperstreamlines(separatrices), three of which lie on the surface $z = -1.05$ in a trisector pattern and the forth, which is pointing in the $+z$ direction, connects the points of triple degeneracy, and delineates one of the two symme-



Figure 5: Stress tensor induced by two compressive forces; minor hyperstreamlines

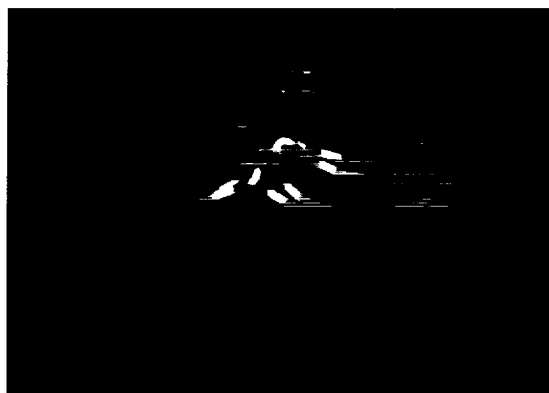


Figure 6: Stress tensor induced by two compressive forces; medium hyperstreamlines

try planes (the other goes through the points of action of the forces).

To further clarify the tensor topology, the skeletons of the minor and medium hyperstreamlines are presented in Figures 5 and 6 respectively. We can see from Figure 5 that the minor hyperstreamlines form a trisector-point like pattern in the vicinity of the points of triple degeneracy. They also indicate that a locus of points of double degeneracy ($\lambda_2 = \lambda_3$) connects the points of triple degeneracy. This is evident from the two trisector points that lie in the symmetry planes just below the points of triple degeneracy. The existence of the line of double degeneracy is further verified by noting the two points of double degeneracy in the skeleton of the medium hyperstreamlines (Figure 6).

5 Conclusions

In this paper, we applied novel methods to determine the topology of tensor data sets, and made use of advanced representations to determine the significance of degenerate points and topological skeletons in terms of physical features.

By extracting the geometric structure of tensor data, we produce simple and austere depictions that allow observers to infer the behavior of any hyperstreamlines in the field. It enables important elements of 3-D stress distribution to be envisaged without visual clutter.

Degenerate points represent the singularities of the tensor field. In the 3-D elastic stress tensor case we were able to identify points of zero stresses with triple degenerate points and to illustrate transmission of forces inside the material.

Acknowledgment

We are most indebted to Rajesh Batra from Stanford University for his critical comments and some of his visualization software. The authors are supported by NASA under contract NAG 2-911 which includes support from the NASA Ames Numerical Aerodynamics Simulation Program and the NASA Ames Fluid Dynamics Division, and also by NSF under grant ECS-9215145.

References

- [1] T. Delmarcelle and L. Hesselink, "Visualization of second-order tensor fields and matrix data," in *Proc. IEEE Visualization '92*, pp. 316-323, CS Press, Los Alamitos, CA., 1992.
- [2] T. Delmarcelle, *The Visualization of Second-Order Tensor Fields*. PhD thesis, Stanford University, 1994.
- [3] J. L. Helman and L. Hesselink, "Visualization of vector field topology in fluid flows," *IEEE Computer Graphics and Applications*, vol. 11, no. 3, pp. 36-46, 1991.
- [4] T. Delmarcelle and L. Hesselink, "Visualizing second-order tensor fields with hyperstreamlines," *IEEE Computer Graphics and Applications*, vol. 13, no. 4, pp. 25-33, 1993.
- [5] T. Delmarcelle and L. Hesselink, "A unified framework for flow visualization," in *Computer Visualization* (R. Gallagher, ed.), ch. 5, CRC Press, 1994.
- [6] H. M. Westergaard, *Theory of Elasticity and Plasticity*. Cambridge, Harvard University Press, 1952.